The Importance of Deposition for Individual and Collective Doses in Connection with Routine Releases from Nuclear Power Plants

Thykier-Nielsen, Søren; Larsen, Søren Ejling

Publication date:
1982

Document Version
Publisher's PDF, also known as Version of record

RISØ-M-2205

THE IMPORTANCE OF DEPOSITION FOR INDIVIDUAL AND COLLECTIVE DOSES IN CONNECTION WITH ROUTINE RELEASES FROM NUCLEAR POWER PLANTS

S. Thykier-Nielsen and Søren E. Larsen

Abstract. Deposition velocities, v_D, and wash-out coefficients, l_g, to be used in different velocity- and Pasquill classes in Denmark are estimated.

The estimated v_D's describe the maximum dry deposition possible, as the surface is assumed a perfect absorber in the considerations. The l_g-values are found corresponding to the average rain intensity, when it rains, within each Pasquill class and apply for materials which dissolve rapidly in water. The estimated parameter values were used as central values in a parameter study as follows:

For four different deposition cases and two release heights the committed effective dose equivalent (individual and collective) from a postulated annual routine release to the atmos-

(continue on next page)

April 1982
Risø National Laboratory, DK 4000 Roskilde, Denmark

phere has been calculated. An increase of the deposition parameters by more than one order of magnitude was found to have negligible influence on the total committed effective dose equivalent. However, the choice of deposition parameters was found to be of major importance for the assessment of the surface contamination and thus the radiological consequences of airborne routine releases.

INIS descriptors: BWR TYPE REACTORS; DEPOSITION; FISSION PRODUCTS; FISSION PRODUCT RELEASE; METEOROLOGY; RADIATION DOSES; WASHOUT

UDC 614.73:614.876:621.039.58

ISBN 87-550-0635-3
ISSN 0418-6435

Risø repro 1982

CONTENTS

1. INTRODUCTION

The deposition velocity is a fairly important parameter when dispersion from nuclear facilities is studied, in connection with safety studies.

The reason for this is that it (together with the washout coefficient) determines the fraction of the released material, that does not blow away, but remains on the surface, and thereby both enters the ecological system and continues to contribute to the doses for much longer time than the material does, that remains airborne.

The effects of deposition of course is most striking in connection with short term (accident) releases, where the difference in residence time between the airborne material and the deposed material is largest. In this study however, we have concentrated on routine releases, to avoid having to concern ourselves with the many and different types of accident releases.

2. EVALUATION OF DEPOSITION

2.1. Micrometeorological considerations

In this section we shall consider the dispersed material as a trace gas in the atmosphere (the considerarions will therefore be valid for gasses and particles of diameters less than 1 μ (Nielsen, 1982). We shall largely follow the considerations presented in Jensen (1981) and Nielsen (1982).

Theoretical estimates of the deposition velocity are based on models of the physical processes in the lowest few meters of the atmospheric boundary layer and on the surfaces. We shall concentrate on the atmospheric processes. Therefore it is convenient to apply the Monin-Obukhov scaling laws to the parameters of interest. We shall consider velocity, u, temperature θ and concentration of a trace gas χ.

The vertical gradients of the mean values of these quantities can be written (Busch, 1973).

$$\frac{kz}{u_*}\frac{\partial \bar{u}}{\partial z} = \phi_M(z/L),$$

$$\frac{kz}{\theta_*}\frac{\partial \bar{\theta}}{\partial z} = \phi_H(z/L), \qquad (1)$$

$$\frac{kz}{\chi_*}\frac{\partial \bar{\chi}}{\partial z} = \phi_\chi(z/L),$$

where

$$u_* = (-\overline{u'w'})^{\frac{1}{2}} \qquad (2)$$

$$\theta_* = -\overline{\theta'w'}/u_* \;,\; \chi_* = -\overline{\chi'w'}/u_*$$

In (2) θ', u', w' and χ' are fluctuations, and w is the vertical velocity.

The parameter L is called the Monin-Obukhov length and is a measure of the importance of the heat flux $\overline{\theta'w'}$. L is defined as

$$L = \frac{\bar{\theta}\, u_*^2}{gk\, \theta_*} \tag{3}$$

If the heat flux goes to zero, L is seen to go to infinity. This situation is called neutral, when L is positive the heat flux goes downwards, and the situation is called stable, L negative on the other hand means upward heatflux, a situation which is called unstable. For $L \to \infty$, $\phi_M(z/L) \to \phi_M(0) = 1$.
This result is ensured by the choice of the von Karman constant, k, in (1). This constant is generally found to be between 0,34 and 0,41.

The general behaviour $\phi_M(z/L)$ is fairly well established (Busch, 1973).

$$\phi_M(z/L) = \begin{cases} (1-\gamma_m\, z/L)^{-1/4} & z/L < 0 \\ 1+\beta_m\, z/L & z/L > 0 \end{cases} \tag{4}$$

The behaviour of $\phi_H(z/L)$ is less well established; it is not even agreed that it goes to 1 for $z/L \to 0$. We define ϕ_H' from

$$\phi_H(z/L) = \begin{cases} \phi_0(1-\gamma_h\, z/L)^{-\frac{1}{2}} \equiv \phi_0\, \phi'_H;\ z/L < 0 \\ \phi_0(1+\beta_h\, z/L) \equiv \phi_0\, \phi'_H;\ z/L > 0 \end{cases} \tag{5}$$

Very few direct measurements exists of $\phi_M(z/L)$ and $\phi_H(z/L)$; from Busch (1973) we can summarize

Table 2.1. Estimates of turbulence constants from suface-layer measurements (Busch, 1973).

Source	γ_m	β_m	γ_h	β_h	k	$\phi_h(0)$
Businger et al.(1971)	15	4.7	9	6.4	0.35	0.74
Paulson (1970) } Badgley et al. (1972) }	16	7	16	7	[0.4]	[1]
Webb (1970)	18+	5.2	9+	5.2	[0.41]	[1]
Dyer and Hicks (1970)	16	-	16	-	0.4	1

Brackets indicate that the value is assumed and fluxes estimated from profiles

+ Webb uses log-linear profiles for a slightly unstable atmosphere ($z/L < -0.03$) and finds a coefficient of 4.5 for both ϕ_m and ϕ_h which leads to $\gamma_m = 18$ and $\gamma_h = 9$. Businger et al. have $\phi_H = 0.74 + 4.7z/L$ for $z/L > 0$.

Even less certainty than exists for $\phi_\chi(z/L)$ than for $\phi_H(z/L)$. It is generally assumed that $\phi_\chi = \phi_H$. However, Nieuwstadt and van Ulden (1978) argues that while this may be true for close to neutral stability, where temperature can be considered a passive scalar, it is not justified in non neutral conditions where buoyancy forces prevail, since the temperature of an airparcel will influence its motion; under such conditions we write for $\phi_\chi(z/L)$

$$\phi_\chi(z/L) = \phi_0 \phi_\chi' , \qquad (6)$$

where we can use either $\phi_\chi' = \phi'_H$ or in according with Nieuwstadt and van Ulden (1978) $\phi_\chi' = \phi_M$.

From (1) we get

$$\bar{u}(z) = \frac{u_*}{k}\left(\ln \frac{z}{z_0} - \psi_M(z/L)\right)$$

$$\bar{\chi}(z) - \chi_0 = \frac{\chi_* \phi_0}{k}\left(\ln\left(\frac{z}{z_\chi}\right) - \psi_\chi(z/L)\right), \qquad (7)$$

where

$$\psi_M(z/L) = \int_{z_0/L}^{z/L} \frac{1 - \phi_m(\xi)}{\xi}\, d\xi$$

$$\psi_\chi(z/L) = \int_{z_\chi/L}^{z/L} \frac{1 - \phi_\chi'(\xi)}{\xi}\, d\xi \qquad (8)$$

and where we have introduced the roughness length z_0 and the corresponding length for χ, z_χ. It is noted that we in (7) have neglected the lower boundary in the integration in (8), in keeping with that one must have $z \gg z_0$ and $z \gg z_\chi$ for application of the Monin-Obukkov hypotheses.

From (2) is seen that the downward flux of χ is given by $-u_*\chi_*$. In modelling approach applying a deposition velocity, v_D, this flux is given as $-v_D\,\chi(z)$. Hence we can estimate v_D from

$$v_D = \frac{u_*\chi_*}{\bar{\chi}} = \frac{k u_*}{\phi_0\left(\ln\frac{z}{z_\chi} - \psi_\chi(z/L) + \frac{k\chi_0}{\phi_0 \chi_*}\right)} \qquad (9)$$

Applying (7) this can be rewritten as

$$v_D = \phi_0^{-1}\, u_* \frac{u_*}{\bar{u}}\left[1 + \frac{u_*}{k\bar{u}}\cdot\ln\left(\frac{z_0}{z_\chi}\right) + \frac{u_*}{k\bar{u}}\cdot(\psi_M - \psi_\chi) + \frac{u_*}{\chi_*}\frac{\chi_0}{\phi_0\bar{u}}\right]^{-1} \qquad (10)$$

with $\phi_0 = 1$ this equation is the basis for the often stated result, that

$$v_D < u_* \frac{u_*}{\bar{u}} \qquad (11)$$

The last term in the bracket reflects that a surface can not always absorb the material, transported down towards it by the turbulence. Indeed, this term is often the dominating term in the denominator. The second term in the bracket is due to the difference between z_0 and z_χ . Generally z_χ is somewhat larger that z_0 for smooth flow conditions (over water, while it for rough flow conditions can be considerably smaller than z_0 (Brutsaert, 1975 , and Garratt and Hicks, 1973). For over water flows this term will therefore enhance the deposition velocity, while it for over land flow will diminish it.

The value og z_0/z_χ does depend both on the trace gas and on the flow situation. For relevant flow situations overland it seems however that the following simple relationship describes the data well (Garratt and Hicks, 1973), where it more specifically is found to apply for both temperature and water vapour.

$$1 < \ln\frac{z_0}{z_\chi} < 3, \qquad (12)$$

with a best overall expression given by the "e^2-law": $z_0/z_\chi = e^2$,

See Figure 2.1.

Next we turn towards the term $\psi_M - \psi_\chi$, which by use of (8) can be written

$$\Delta\psi = \psi_M(z/L) - \psi_\chi(z/L) = \int_0^{z/L} \frac{\phi_\chi' - \phi_M}{\xi} \, d\xi \qquad (13)$$

The behaviour of this term obviously will depend somewhat on which formulas we use to describe the ϕ-functions.

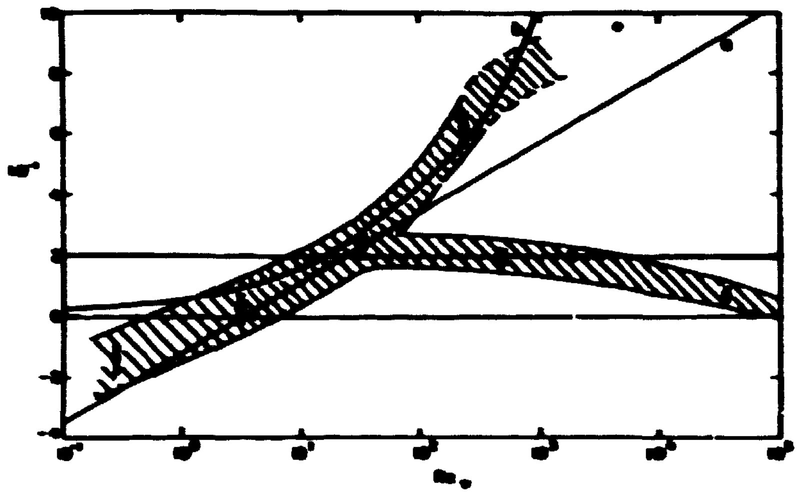

<u>Fig. 2.1.</u> The overall behaviour of $kB^{-1} = \ln z_0/z_T$ with $Re_* = u_* z_0/\nu$. Typical over water flows have $Re_* \sim 1$ while typical over land flows have $10^2 < Re_* < 10^4$. The shaded bands represent 95% confidence limits (Garrat and Hicks, 1973).

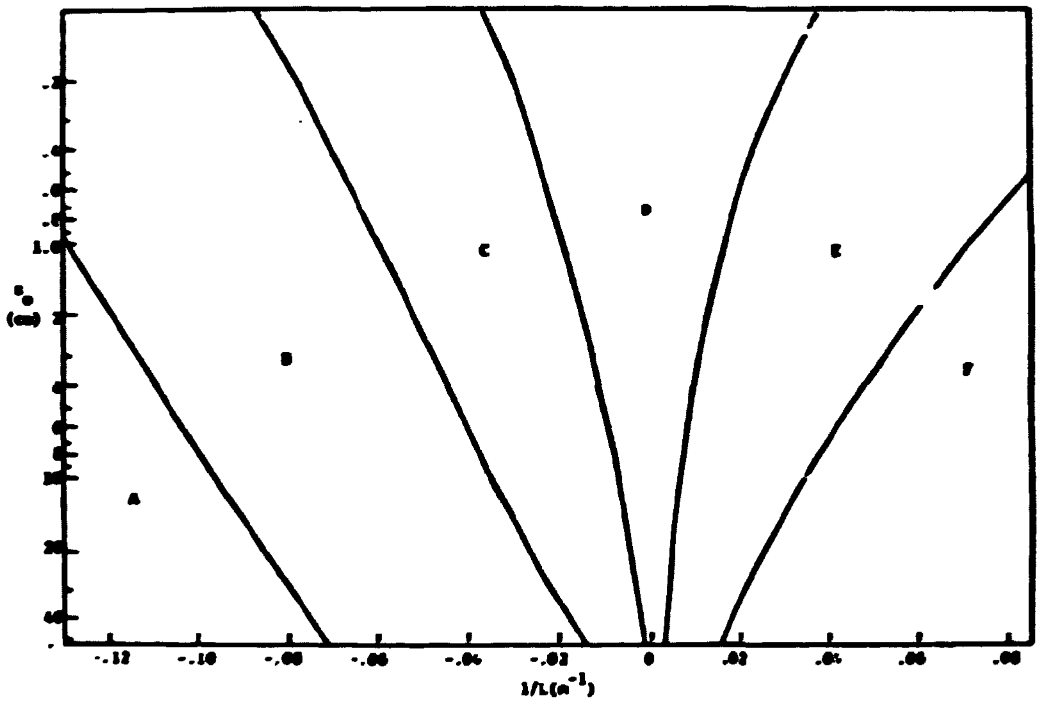

<u>Fig. 2.2.</u> Empirical relation between the Monin Obukhov length, L, and the Pasquill dispersion classes for different z_0-values (Golder, 1972).

In table 2.2 the behaviour of (13) is described for some of the data sets in table 1 and with ϕ_χ' equal to either ϕ_H' or ϕ_M.

Table 2.2. Behaviour of (13) for the different data sets from table 2 and for different assumptions for ϕ_χ.

Data set	ϕ_0	ϕ'_χ	$\Delta\psi(z/L>0)$	$\Delta\psi(-2<z/L<0)$
Businger et al. (1971)	0.74	ϕ_H'	1.7 z/L	$\sim -0.36\ (-z/L)^{\frac{1}{2}}$
	0.74	ϕ_M	0	0
Paulson(1970) and Dyer and Hicks (1970)	1	ϕ_H'	0	$\sim -0.8(-z/L)^{1/3}$
	1	ϕ_M	0	0
Webb (1970	1	$\phi H'$	0	$\sim -0.3(-z/L)^{\frac{1}{2}}$
	1	ϕM	0	0

From table 2 and (10) it can be seen that the upper bound for V_D can be stated as

$$v_D < \phi_0^{-1}\, u_* \frac{u_*}{\bar{u}}\left(1 + \frac{u_*}{k\bar{u}}\ln\frac{z_0}{z_\chi}\right)^{-1} \quad \text{for } z/L > 0$$

$$v_D < \phi_0^{-1}\, u_* \frac{u_*}{\bar{u}}\left(1 + \frac{u_*}{k\bar{u}}\left(\ln\frac{z_0}{z_\chi} - \alpha\right)\right)^{-1} \quad \text{for } z/L < 0, \tag{14}$$

where α depends on stability and on the chosen ϕ-functions. Since v_D is to be estimated fairly close to the ground, a reasonable guess on the extremum z/L-value of interest is $1 > z/L \gtrsim -1$, meaning that α is bounded as

$$0 < \alpha < 0.8 \tag{15}$$

Although the majority of the models in table 2 would put α closer to zero than 0.8, the combined uncertainty on $\ln(z_0/z_\chi)$ and α suggests to use the following expression for $z/L<0$ for flows over land.

$$v_d < \phi_0^{-1} u_* \frac{u_*}{\bar{u}} \qquad z/L < 0 \qquad (16)$$

The last parameter uncertainty, we wish to discuss, is associated with the choice of ϕ_0 and k. As will be discussed in section 3 our primary aim is to calculate the upper bounds for v_D from knowledge about the velocity, u(z), and the stability.

By means of (7) we can write the leading term in (14) and (16) as

$$\phi_0^{-1} u_* \frac{u_*}{\bar{u}} = \frac{k^2 \bar{u}(z)}{\phi_0} \left(\ln\left(\frac{z}{z_0}\right) - \psi_M(z/L) \right)^{-2} \qquad (17)$$

From table 1 is seen that the data sets in the litterature give (k, ϕ_0) as (0.35, 0.74) or as (0.4-0.41, 1), which shows that $k^2\phi_0^{-1}$ is essentially independent on which values of (k, ϕ_0) we believe in. In the further study we will use $(k, \phi_0)=(0.4,1)$. Note finally that the correction term in (14) can be written

$$\frac{u_*}{k\bar{u}} = \left(\ln \frac{z}{z_0} - \psi_M(z/L) \right)^{-1}$$

which is again independent on the choice of k-value.

As discussed by Jensen (1981) the height dependency of v_D implies that $\bar{\chi}$ and v_D have to pertain to the same height above the ground, when the deposition is calculated. For the practical use of the estimated v_D it is therefore reasonable to calculate v_D at such a height that $z >> z_0$, whereby v_D becomes a slowly varying function of height and the precise height to which it pertains becomes less critical. Furthermore, as discussed above, the application of the Monin-Obukhov scaling demands that $z>>z_0$ or at least $z \gtrsim 5z_0$.

After these more theoretical considerations we now turn to estimates of the upper bounds for v_D pertaining to the dispersion class statistics obtained by Jensen (1973) on basis of data from the Risø Meteorology tower.

2.2. Upper bounds on the deposition velocity.

On basis of 10 years of hourly data from the Risø meteorological tower Jensen (1973) has compiled a three dimensional distribution function for wind direction, wind speed and Pasquill class, where the Pasquill class is estimated on basis of the vertical temperature gradient over the lowest 100 meter of the atmosphere, while the wind speed and direction derives from measurements 123 m above the surface.

The wind direction needs not to concern us here. The velocity classes and Pasquill classes are specified as given in table 2.3.

Table 2.3. Specification of velocity and Pasquill classes according to Jensen (1973). The estimated mean parameters denoted by <> for each class are introduced for later use. The estimates of the reciprocal Monin-Obukhov length, L, are described later.

Velocity classes		Pasquill stability classes			
U_{123} [m/s] interval	$\langle u \rangle_{123}$ [m/s]	Pasquill class	ΔT-interval [°C/100 m]	$\langle \Delta T \rangle$ [°C/100 m]	$\langle 1/L \rangle$ [m^{-1}]
u<1	0.5	A	<-1.9	-2	-0.12
1 < u<3	2	B	1.9<ΔT<-1.7	-1.8	-0.07
3 < u<6	4.5	C	1.7<ΔT<-1.5	-1.6	-0.02
6 < u<10	8	D	-1.5<ΔT<-0.5	-1.0	0
u > 10	11.5	E	-0.5<ΔT<1.5	0.5	0.02
		F	1.5<ΔT<4	2.75	0.07

To relate the classification scheme in table 3 to the conditions in the lowest few meters of the atmosphere, we shall appeal to a study of the Risø mast data described in Mahrt et al. (to be published).

They found that the velocity profile along the tower were well approximated by

$$u(z) = u_{\infty} \left(c_b \ln\left(\frac{z}{z_0}\right) e^{-z/H} + 1 - e^{-z/H}\right), \qquad (19)$$

Where u_{∞} is the wind aloft, here u_{123}, i.e. the velocity used in table 3, c_b is a drag coefficient, while H is a scale height. The two last coefficients were found to be stability dependent through a bulk Richardson number, Ri_B, given by:

$$Ri_B = \frac{g}{T} \frac{(T_{112}-T_2+1,07)}{u^2_{117}} \qquad (20)$$

The relations between c_b,H and Ri_B are given in table 2.4.

Table 2.4. c_b and H as function of Ri_b

Ri_B	$Ri_B<-0.03$	$-0.03<Ri_B<-0.005$	$0.005<Ri_B<0.005$	$0.005<Ri_B<0.25$	$0.25<Ri_B$
c_b	0.13	0.12	0.11	0.084	0.01
H[m]	75	77	81	56	30

In the same study was found that the roughness length most characteristical for the Risø tower data was

$$z_0 = 5 \text{ cm} \qquad (21)$$

The procedure is now: By means of (19,20) and tables 2.3 and 2.4 U_{123} is extrapolated down to yield u_{10}, where indices refer to height above ground. Based on this value for u_{10} the other parameters of interest was estimated by use of the formulas in section 2.2.

For stable conditions $v_{D,max}$ was determined from

$$v_{D,max} = u_* \frac{u_*}{\bar{u}(z)} \left(1 + \frac{u}{k\bar{u}} \ln \frac{z_0}{z_\chi}\right)^{-1} \qquad (22)$$

For unstable conditions

$$v_{D,max} = u_* \frac{u_*}{\bar{u}(z)} \qquad (23)$$

$\mathrm{Ln}(z_0/z_\chi)$ was set to 1 compare (12) and $u_*/\bar{u}(z)$ was determined from (17) with $k = 0.4$ and $\psi_M(z/L)$ chosen according to (14) with the parameter values after Businger et al. (1971), in table 2.1. The z/L-values corresponding to the different Pasquill classes were chosen on basis of the work by Golder (1972), see Figure 2.

The values for L^{-1} are shown in table 3. The actual form of ψ_M are based on the results of Paulson (1970) with the exception of that the newer parameter values of Businger et al. (1971) are substituted for the parameter used by Paulson.

$$\psi_M(z/L) = 2 \ln\left(\frac{1+x}{2}\right) + \ln\left(\frac{1+x^2}{2}\right) - 2 \arctan(x) + \pi/2; z/L < 0,$$

$$\psi_M(z/L) = -4.7\ z/L \text{ for } z/L > 0 \qquad (24)$$

$$x = (1-15\ z/L)^{1/4}$$

The resulting values for $v_{D,max}$ are listed in table 2.5.

Table 2.5. Maximum possible deposition velocities v_D [cm/s] for the different dispersion categories described by Jensen (1973). The values are estimated as described in the text. The upper values pertain to z = 2 m while the lower values pertain to z=10 m. The velocity classes are based on windspeed at 123 m above ground. The numbers are based on a roughness length, z_0 = 5 cm.

Pasquill class / velocity class	A	B	C	D	E	F	Height, z [m]
	0.45	0.39	0.33	0.21	0.08	0.06	2
u < 1 m/s	0.35	0.30	0.24	0.15	0.06	0.03	10
	1.80	1.59	1.33	0.81	0.33	0.22	2
1m/s<u<3m/s	1.40	1.21	0.98	0.61	0.22	0.12	10
	4.07	3.58	3.01	1.83	0.76	0.50	2
3m/s<u<6m/s	3.16	2.73	2.21	1.37	0.52	0.28	10
	7.25	6.38	5.02	3.26	2.25	0.90	2
6m/s<u<10 m/s	5.65	4.85	3.69	2.43	1.52	0.50	10
	10.44	8.58	7.21	4.69	3.24	2.14	2
10m/s<u	8.11	6.52	5.30	3.50	2.19	1.12	10

The method used in arriving to the deposition velocities are somewhat complicated owing to the complex terrain around the Risø tower and to that the basis height 123 m is above the surface layer, where the formulas in section 2.2 apply, see Fig.2.3. Due to these complexities the profile relationship given by (19,20) with table 2.4 yields a better description of the velocity profiles than the Monin Obukhov similarity expressions of section 2.2. Owing to the simplicity of (19), this equation must on the other hand be expected to give a less precise description of the behaviour of a surface layer flow than the Monin-Obukhov expressions, on which the formulas for v_D are based.

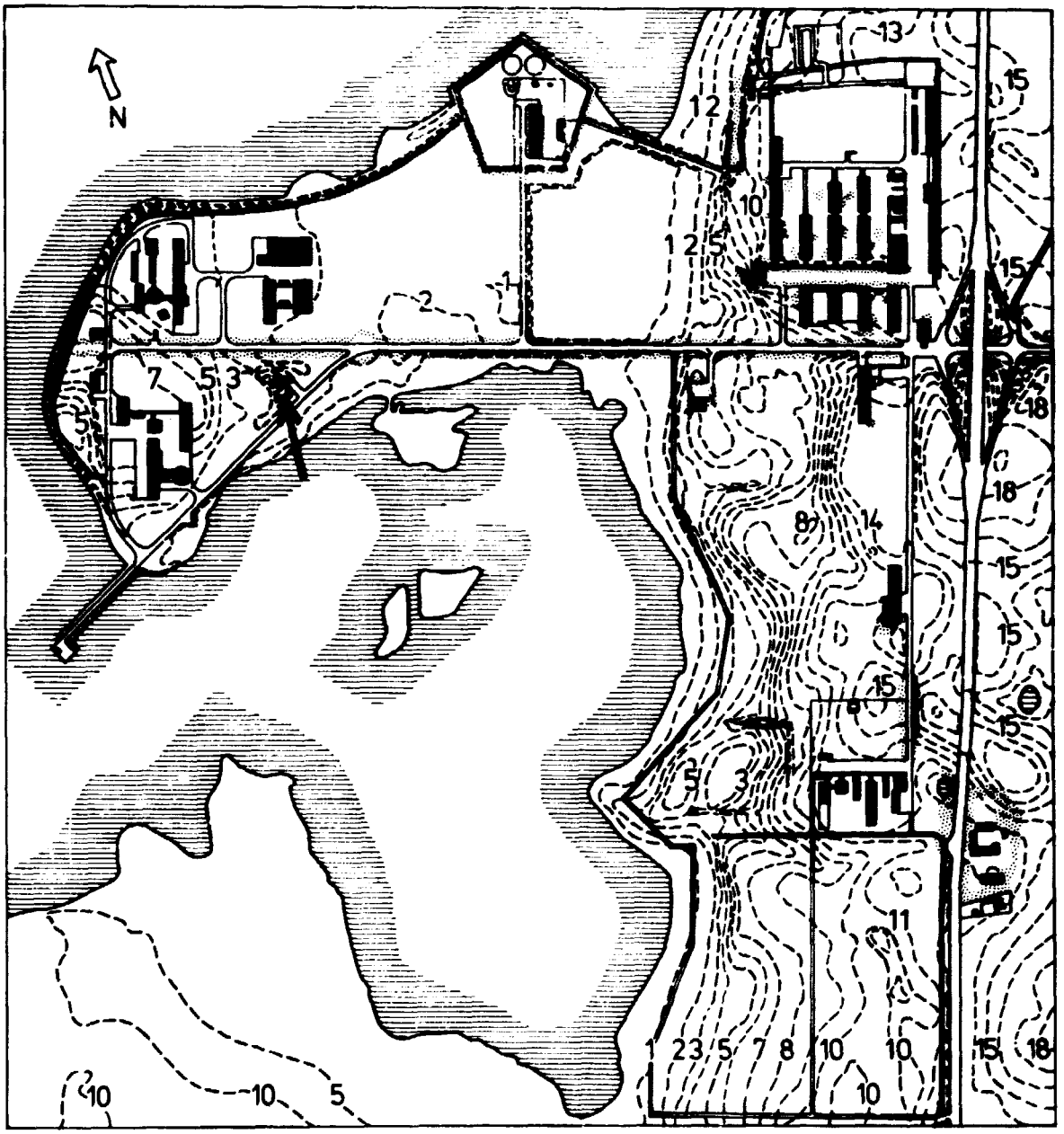

Fig. 2.3. Map of Risø, showing the position of the meteorology tower (indicated by +) on the peninsula surrounded by laboratory buildings.

Also, it must of course be emphasised that the appearance of very (un)stable situations associated with very high velocities in table 2.5 is somewhat formal, in the sense that these combinations appears very rarely in the data, meaning that although the combination exists in the table it has little weight in dispersion calculations based on the statistics in Jensen (1973).

Finally it should be repeated again that the $v_{D,max}$ values in table 2.5 are absolute maximum values for v_D since the term $u_* x_0/(\chi_* \phi_0 \tilde{u})$ in (10) has been neglected and the other terms in the denominator are underestimated. In his review of the existing data on deposition velocities Nielsen (1981) concludes, that for the here relevant types of material deposition velocities are unlikely to exceed 2 cm/s. In his relation the values in table 2.5 simply indicate that v_D = 2 cm/s will only be possible in certain dispersion categories, i.e. the categories in table 2.5, where $v_{D,max}$ is larger than 2 cm/s.

Based on this discussion and table 2.5 we can therefore establish a new set of recommended maximum depostion velocities pertaining to the height interval between 2 and 10 m and the roughness length equal to 5 cm. These velocities are given in table 2.6, which simply consist of the values from table 2.5 averaged between 2 and 10 m and bounded from above by 2 cm/s.

Table 2.6. Recommended maximum v_D-values pertaining to z_0 = 5 m and the height 2-10 m, and to the different dispersion categories in Jensen (1973). Unit [cm/s] .

Pasquill class / velocity class	A	B	C	D	E	F
u < 1m/s	0.4	0.3	0.3	0.2	0.07	0.05
1m/s<u<3m/s	1.6	1.4	1.2	0.7	0.3	0.3
3m/s<u<6m/s	2.0	2.0	2.0	1.5	0.6	0.4
6m/s<u<10m/s	2.0	2.0	2.0	2.0	1.8	0.6
10m/s<u	2.0	2.0	2.0	2.0	2.0	1.6

2.3. Estimation of wash-out coefficients

In the case of precipitation there is a wet removal of effluents. Usually one distinguishes between below-cloud scavenging, denoted wash-out, and within-cloud scavenging or rain-out. Rain-out removes the material from the plume, and causes unpredictable deposition patterns dependent on where and if the clouds involved will rain. In general this phenomenon will act to reduce concentrations within the plume without neccesary causing deposition below it. We shall neglect rain-out.

Wash-out is usually parametrised by use of a wash-out coefficient, l_g. It is defined as the rate of change of concentration per unit time, due to wash-out, i.e.

$$\chi' = \chi \cdot \exp(-l_g x/u), \qquad (1)$$

where χ' and χ are concentrations with and without washout, x is distance to source and u the mean advection speed of the plume.

For a gas the wash-out coefficients depends on the solubility of the gas in water and the time constant of the dissolving process. From Figure 5.11 in Engelmann (1968) one obtains Table 2.7.

Table 2.7.

Rain intensities [mm/hr]	0.06	0.1	0.5	1	3	10	100
l_g [sec^{-1}]	10^{-5}	$1.3 \cdot 10^{-5}$	$3 \cdot 10^{-5}$	$4 \cdot 10^{-5}$	10^{-4}	$2 \cdot 10^{-4}$	10^{-3}

Table 2.7 is based on a diffusitivity of gas in air of D= 0.1 m^2/s. The values in the table are found to describe l_g fairly well for gases that dissolve fast in water. It actually pertains to the very active gas of Bromine.

For particles, the wash-out efficiency depend on particle size and rain drop size distribution. Since the latter is found to relate to rain intensity, the washout efficiency for particles can be given in terms of rain intensity as well. For particles less than a few microns in diameter Table 2.7 is found to apply. Bryant (1966) argues that ^{90}Sr and ^{137}Cs will be present in this particle size range in routine releases from a nuclear plant.

Important effluents from nuclear power plants are organic and inorganic Iod-gases. For inorganic Iod-gases Beattie and Bryant (1973) find l_g between $3 \cdot 10^{-6}$ sec^{-1} and $2 \cdot 10^{-7}$ sec^{-1} for rain while Engelman (1968) gives values around $5 \cdot 10^{-8}$ sec^{-1} for snow.

For organic compounds like CH_3I Engelman (1968) found values which are about 1% of the above given values.

The reason why l_g is smaller for I_2-gases than indicated by table 2.7 is the slow rate of dissolution in water for these gases. For CH_3I the reason is more straight forward that this gas essentially does not dissolve in water.

The quoted reduction in l_g for snow relative to rain is quite general and usually corresponds to a factor between 2 and 10 (Engelmann, 1968, Gyllander and Widemo, 1980, Nielsen, 1981).

In the following we shall estimate l_g values to be used in connection with computation of yearly average concentrations (and doses) in Denmark. We shall concentrate on gases (or particles) for which table 2.7 apply. Our approach will be to estimate the frequency of rain in each Pasquill stability category, see section 2.2, and the average rain intensity, when it rains.

Unfortunately we do not have a study for Denmark which is comprehensive enough to yield the numbers, we need. Therefore we shall combine 3 different studies and data sets to obtain the necessary estimates.

The 3 different data sets pertain to Carnsore Point in southern Ireland, Risø and Studsvik, 100 km south of Stockholm. The data from the first location is analysed by Jensen et al. (1982) while the results from the two last locations are taken from Gyllander and Widemo (1980).

For the three locations the total distribution of stability categories is

Table 2.8. Distribution of stability [% of time] at Carnsore Point, Risø, and Studsvik. The stability at Carnsore Point is determined by a combination of a net radiation index and the wind speed. The stability at Risø and Studsvik is determined from the ΔT-method described in section 2.2.

Stability	A	B	C	D	E	F+G	Total
Carnsore	0.3	1.9	4.6	81.2	8.0	4.00	100
Risø	1.2	1.7	3.3	60.3	27.1	6.5	100
Studsvik	0.9	1.0	2.1	50.7	35.0	10.3	100

The difference in stability distribution for the three locations reflects partly climatological differences partly differences in the different schemes for stability determination.

It is well known from the litterature e.g. Kretzschmar and Mertin (1980) that the ΔT-method tend to increase the probability of class E and decrease the probability of class D relative to the radiation/windspeed method; indeed it is seen that the probability of (D plus E) is about the same for all locations (89.2% for Carnsore, 87.4% for Risø and 85.7% for Studsvik).

From a climatological point of view Carnsore Point is very much in the temperate maritime region, so is Risø but closer to the European land mass. Studsvik comes even closer to a continental climate and is further north as well. For Studsvik it is seen that this means that the stability distribution is moved somewhat more towards stable conditions that the Risø distribution.

For the three data sets the occurrences of precipitation in per cent of time within a given class is found to be

Table 2.9. Probabilities of a given rain intensity within a stability class [% of time in class] and in total [% of time] for Carnsore, Studsvik and Risø. Precipitation is defined to occure when more than 0.1 mm/hr is measured.

		A	B	C	D	E	F+G	Total
Carnsore	0.1-1mm/hr	0.0	1.0	2.2	10.8	1.4	1.8	9.1
Point	1-5 mm/hr	0.0	0.2	0.5	4.2	0.3	0.3	3.5
	5-10 mm/hr	0.0	0.0	0.01	0.12	0.01	0.02	0.1
	> 0.1mm/hr	0.0	1.1	2.7	15.2	1.6	2.1	12.7
Studsvik	> 0.1mm/hr	0.8	1.8	2.0	9.7	7.4	2.7	7.7
Risø	> 0.1mm/hr							7.2

The Carnsore data covers the period 1957-1978 and the Studsvik data the period 1960-64. For Risø the stability is determined for the period 1958-68, while the precipitation is obtained from 7 years of data 1970-75 and 1978. The fact, that these data are not yet on a computer compatible form, tells why the Risø statistics are not filled in on Table 2.9. This is the main reason for the effort to use Studsvik and Carnsore data to estimate the missing Risø information.

From Table 2.9 is seen that the probability of rain in stability classes, A,B,C, and F+G is very much alike for Studsvik and Carnsore. The main differences are found in stability class group D+E. The probability of these groups were above found to

be about the same for the three data sets.

The contributions to total probability of precipitation for Carnsore and Studsvik from stability classes D+E

Carnsore (15.2·81.2 + 1.6·8.0)/100 = 12.5%

Studsvik (9.7·50.7 + 7.4·35.0)/100 = 7.5%,

which shows that the differences in the precipitation probability for the two stations can be exclusively attributed to differences between the frequency of precipitation in the two stability classes D and E. This latter difference in all likelyhood is of climatic nature in that frontal systems are expected to be much more vigorous at Carnsore Point that at Studsvik. This argument is strengthed by that the probability of precipitation within each category are so alike for classes A,B,C and F+G.

The similarities and differences between the three locations can further be illuminated by considering the probabilities of a given rain intensity for the situations with precipitation larger than 0.1 mm/hr.

Table 2.10. Cumulated distribution of precipitation intensities at Studsvik, Risø and Carnsore Point [% of time with precipitation] . The table is compiled from Jensen et al (1982) and Gyllander and Widemo (1990). The probability of 0.1 ≤ p<1 for Studsvik is missing because of the low sensitivity of the Studsvik rain range.

Precipitation intensity, p [mm/hr]	Studsvik	Risø	Carnsore
0.1 ≤ p<1	-	18.40	58.10
0.1 ≤ p<2	92.50	93.50	76.90
0.1 ≤ p<3	97.43	97.03	89.10
0.1 ≤ p<4	98.26	98.48	94.50
0.1 ≤ p<5	99.12	99.00	96.71
0.1 ≤ p<6	99.44	99.23	98.06
0.1 ≤ p<7	99.73	99.52	98.68
0.1 ≤ p<8	99.79	99.64	99.05
0.1 ≤ p<9	99.85	99.71	99.33
0.1 ≤ p<10	99.94	99.77	99.50

Table 2.10 shows that the probability of higher precipitation intensities is largest at Carnsore, lowest at Studsvik with Risø in between. For the bulk of the precipitation p<5 mm/hr the distributions are very similar for Risø and Studsvik. From Table 2.9 it is seen that the higher precipitation intensities are most likely to occur in class D at Carnsore, a fact which add further credibility to the argument above, that the difference in total probability of precipitation at Studsvik and Carnsore is mostly due to differences in rain probability in the group (D+E), where we have combined D and E to compensate for the differences in stability determination schemes.

Based on the above discussion we shall consider the Risø distribution of precipitation in stability classes to be very similar to Studsvik's, but it must result in a total precipitation probability of 7.2% rather than 7.7%, and the differences in distribution of stability classes must be included, so must also the knowledge that the Risø statistics are a bit closer Carnsore's than Studsvik's are. As a result we postulate the following distribution of precipitation and dry weather in stability classes at Risø.

Table 2.11. Postulated distribution of dry weather and precipitation for Risø for each stability class and in total.

Stability	A	B	C	D	E	F+G	Total
Precipitation [% of time in class]	0.5	1.5	2.5	9.5	4.5	2.5	7.2
Dry weather [% of time in class]	99.5	98.5	97.5	90.5	95.5	97.5	92.8

Next we shall estimate the average precipitation intensities for each stability class. Integrating the distributions for Carnsore Point we obtain:

Table 2.12. Average precipitation intencity when precipitation occurs at Carnsore Point, estimated from the distributions in Table 2.9.

Stability	A	B	C	D	E	F+G	Total/year
Mean precipitation intensity [mm/hr]	-	1.39	1.46	1.80	1.43	1.32	1986 m
Intensity of class relative to intensity of class D	-	0.77	0.81	1	0.79	0.73	-

The total precipitation in Table 2.12 is estimated from the mean intensities and the occurrences of precipitation and stability classes and it is too high. In Jensen et al. (1982) the average precipitation at Carnsore Point is estimated to approximately 1000 mm/year. The reason for this overestimation is that the discrete form of the distributions in Table 2.9 are too coarse to yield an accurate estimate. Never the less we shall assume that the relative intensities between classes as depicted by Table 2.12 are valid. They reflect that high intensity rain is most probable under neutral conditions and least probable under stable conditions. This is clearly reflected in Table 2.9 and makes physical sense as well. From Larsen and Jensen (1982) is found that the yearly average amount of precipitation in Denmark is 767 mm. With this figure and the above information about relative precipitation intensity between classes, distribution of precipitation and dry weather in classes and distribution of stability classes we can estimate the mean precipitation intensites at Risø. We assume that the relative intensity in class A is 0.77, corresponding to class B.

Finally we shall discuss the influence of snow. Table 2.14 shows the distribution of rain and snow during the year (Allerup and Madsen, 1979). Table 2.15 shows the corresponding variation of stability classes for the year, based on Risø data for the period 1958-67.

From these two tables are seen that 11.3% of the total yearly precipitation falls as snow during the winter period where the unstable stability classes are virtually absent. Therefore it seems sensible to assume that the snow falls in classes D, E, and F+G. For the lack of more knowledge we assume that the snowfalls constitute 11.5% of the precipitation in each stability class, giving rise to the mean snow frequency indicated in table 2.13. The average l_g value is finally found by a weighted average of the l_g-value corresponding to rain and the l_g-value corresponding to snow. The latter is assumed to be roughly 10% of the l_g-value corresponding to the same water equivalent rain. The resulting rounded off values are given in table 2.13.

Table 2.13. Estimates of average precipitation rates when precipitation occurs for the different stability classes. The associated l_g values are based on Table 2.7.

Stability	A	B	C	D	E	F+G	Total
Frequency [%]	1.2	1.7	3.3	60.3	27.1	6.5	100%
Precipitation	0.5	1.5	2.5	9.5	4.5	2.5	7.3%
Dry weather [%]	99.5	98.5	97.5	90.5	95.5	97.5	92.7%
Mean precip. rate [mm/hr]	0.97	0.97	1.03	1.26	1.00	0.92	767mm/year
l_g [sec^{-1}]	$3.9 \cdot 10^{-5}$	$3.9 \cdot 10^{-5}$	$4.1 \cdot 10^{-5}$	$4.8 \cdot 10^{-5}$	$4.0 \cdot 10^{-5}$	$3.8 \cdot 10^{-5}$	
Mean snow frequency [%]	0.00	0.00	0.00	1.1	0.5	0.3	
l_g corrected for snow [sec^{-1}]	$3.9 \cdot 10^{-5}$	$3.9 \cdot 10^{-5}$	$4.1 \cdot 10^{-5}$	$4.4 \cdot 10^{-5}$	$3.6 \cdot 10^{-5}$	$3.5 \cdot 10^{-5}$	

Table 2.14. Distribution of rain and snow in mm rain equivalent for the different months (Allerup and Madsen, 1982).

	Jan.	Feb.	Mar.	Apr.	May	Jun.	Jul.	Aug.	Sep.	Oct.	Nov.	Dec.	Year
Rain [%]	59	56	57	93	100	100	100	100	100	100	97	76	88.7
Snow [%]	41	44	43	7	0	0	0	0	0	0	3	24	11.3

Table 2.15. Occurences [%] of the different stability classes throughout the year. The Figures are based on the ΔT-system and Risø data for the period 1958-67.

Pasquill category	Jan.	Feb.	Mar.	Apr.	May	Jun.	Jul.	Aug.	Sep.	Oct.	Nov.	Dec.	Year
A	0.0	0.0	0.4.	1.8	3.5	6.0	2.4	0.7	0.2	0.0	0.0	0.0	1.2
B	0.0	0.0	0.7	2.7	4.7	6.6	4.2	1.5	0.7	0.2	0.0	0.0	1.7
C	0.0	0.1	2.9	6.6	8.3	9.3	7.5	3.5	2.5	0.6	0.0	0.1	3.3
D	51.6	53.5	67.8	65.1	60.3	55.2	63.1	64.0	62.9	61.8	62.0	53.1	60.3
E	42.4	39.0	23.7	18.8	17.5	16.4	17.7	24.3	26.3	27.1	32.6	39.8	27.1
F	4.7	7.3	3.9	4.6	5.4	5.9	4.7	5.7	6.9	8.4	5.0	5.8	5.7
G	1.3	2.1	0.6	0.2	0.7	0.7	0.4	0.3	0.4	2.0	0.3	1.1	0.8

The determination of the final figures in table 2.13 has been so involved that it deserves a discussion. One could with some justification claim that this was a lot of paperwork simply because 7 years of precipitation data were not on a form that allowed to determine the frequency of precipitation and its mean rate directly for the different stability categories. However during the arguments presented here, we have obtained additional useful information.

a) That the frequency of precipitation within classes is very similar for two stations as Studsvik and Carnsore Point for the classes A,B, C, and F+G. This in spite of that the stability classes were determined by different schemes.

b) The difference in frequency between the two stations seems to be concentrated in classes D and E, partly reflecting the different schemes and partly the different climates.

c) Also the similarities in precipitation frequencies have been shown between Studsvik and Risø

In summary we have found some credibility for the suggested precipitation statistics in Table 2.13, to be valid in a larger region than the surroundings of Risø, and it seems very unlikely that the table will change much when the Risø precipitation data become directly integrated in the dispersion meteorological statistics at Risø.

It should finally be emphazised that modelling of washout through one coefficient can be a first step only. The final step must be to build i the precipitation distribution with associated l_g in the dispersion calculations.

Even when this is done the basic problem remains of introducing an often strongly inhomogeneous and instationary rain field into the principally stationary Gaussian plume models.

3. ASSUMPTIONS FOR DOSE CALCULATIONS

3.1. Reactor Surroundings

A typical Danish potential reactor site was chosen. The average population density is about 100 persons/km^2. Most of the population is scattered among small and medium size towns (up to 20.000 inhabitants), rural villages and farms.

About 35 kilometers from the site there is a major population centre which has about 250.00 inhabitants.

The population as function of distance from the site is shown on Fig. 3.1.

3.2. The Reactor

The reactor is a boiling water reactor of 3000 MW_{th}, corresponding to 1000 MW_e. This size was chosen because it was used in earlier Danish studies.

3.3. Fission Product Release

The magnitude and composition of the assumed annual routine release is shown in table 3.1. The release rate is assumed to be constant throughout the year. The data for the release has been derived from an earlier Danish study (not published).

The release data given might not be in accordance with more recent experience on routine releases from BWR's and should thus only be considered as rough estimates of actual release data.

Table 3.1. Annual routine fission product release from a BWR.

Isotope	Amount (Curie)
Kr 83m	320
Kr 85m	13000
Kr 85	260
Kr 87	940
Kr 88	9000
Kr 89	5400
Sr 89	0.035
Sr 90	0.0025
I 131	2.1
I 132	19.2
I 133	12.2
I 134	34.4
I 135	17.3
Xe 131m	180.0
Xe 133m	590.0
Xe 133	61000.0
Xe 135m	1800.0
Xe 135	400
Xe 137	9500
Xe 138	5600
Cs 134	0.0018
Cs 137	0.0028
Cs 138	2.1

Population distribution. Gylling Naes.

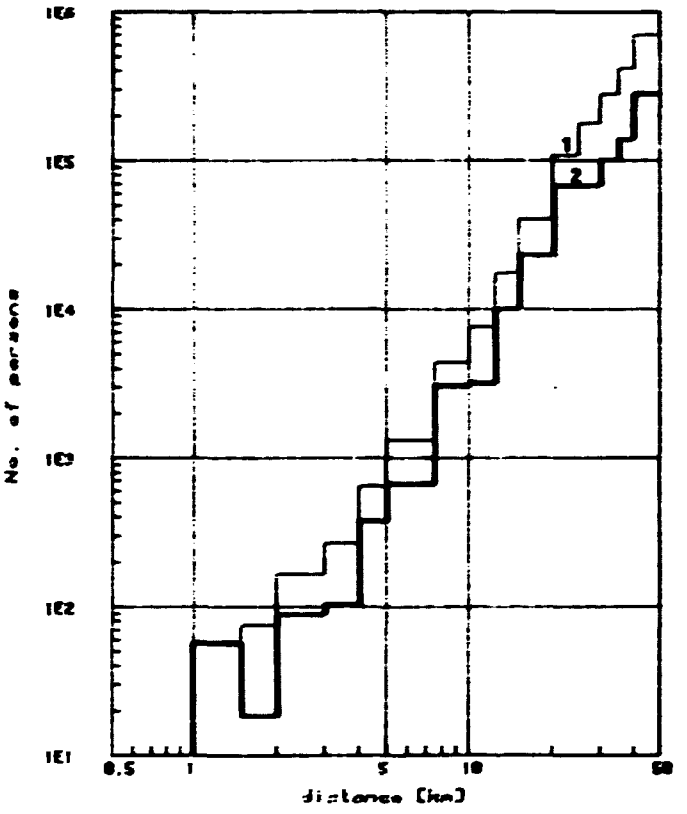

Resident population based on 1992 prognosis.

Seasonal variations included out to 5 km from site.

1. Accumulated pop.
2. Population in distance intervals.

Fig. 3.1

3.4. Dosimetric model

The Risø dose-consequence model, PLUCON2, has been used for the calculation of individual and collective doses.

The dispersion model used in PLUCON2 is the so-called Gaussian model. In this model it is assumed that the material released to the atmosphere will be carried with the wind and spread like a smoke plume. The most important atmospheric parameters are the wind direction, wind speed, and vertical temperature gradient because these determine the transport direction, dilution at the moment of release, and turbulent mixing.

The Gaussian model has been verified out to distances of 5 to 15 km where it is able to predict doses and concentrations within a factor of 2 - 3. At larger distances, doses and concentrations normally are overestimated. This overestimate can be as large as a factor of 10 at 50 km.

In the model both dry deposition and wash-out of the material in the plume is taken into consideration. Dry deposition is calculated according to the source depletion model.

The total dose to an individual is calculated as the sum of three dose components:

Inhalation dose
External gamma dose from the plume
External gamma dose from material deposited on the ground.

The collective dose within a given area is calculated as the sum of the doses to the individuals within the area. Collective doses have been integrated out to 50 kilometers from the plant site. A detailed description of PLUCON2 is given in Thykier-Nielsen (1980).

3.5. Meteorological parameters

Meteorology statistic

The calculations of individual and collective doses from one years routine release of radioactive material are based on Risø meteorological statistics from the period 1958 to 1967 (see Jensen, 1973). Data for the distribution of wind direction, atmospheric stability and wind speed at the height 123 meters above ground level is used.

In the calculations of doses the wind speed at the level of the actual plume height is used, that is the wind speed data from the meteorological statistics which are corrected according to the wind velocity profile at Risø.

The stability is classified in the six Pasquill categories A-F. Turners values for the dispersion parameters, σ_y and σ_z, are used. Crosswind-integrated values of doses are calculated using a sector width of 30 degrees (Thykier-Nielsen, 1980).

Mixing heights according to Klug (1969) are used. The values are given in table 3.2 below.

Table 3.2. Mixing heights for Pasquill stability categories according to Klug (1969).

Pasquill category	A	B	C	D	E	F
Mixing height [m]	1500	1500	1000	500	200	200

The distribution of precipitation and dry weather on stability classes are as given in table 2.13 in section 2.3.

Deposition parameters

Calculations of doses are made for 4 deposition cases as shown in table 3.3 - 3.6:

a. Minimum deposition.
   The minimum value for the dry deposition parameter was chosen according to Nielsen (1981), v_d = 0.01 cm/s.
   For wet deposition (precipitation scavenging) $l_g = 2 \cdot 10^{-7}$ sec^{-1} was chosen as a minimum value.

b. Normal deposition.
   Two cases are considered. In the first case it is assumed that the value of v_d will not exceed 1 cm/s i.e. the values of table 2.6 are used provided they are lower than 1 cm/s and v_d = 1 cm/s elsewhere. This case is denoted "normal deposition 1". In the second case, denoted "normal deposition 2", the values given in table 2.6 of section 2 are used. These values imply a maximum value of v_d = 2 cm/s (according to Nielsen (1981)).

c. Maximum deposition.
   For the sake of comparison a postulated maximum deposition case is studied. For all stabilities and windspeeds the value of v_d is postulated to be 5 cm/sec. The value of l_g is postulated to be $1 \cdot 10^{-4}$ sec^{-1}.

Dry deposition is calculated according to the source depletion model. Alle the values of v_d are regarded as pertaining to the height 10 meters.

Alle isotopes except the noble gases are assumed to be depositable. The deposition parameters are assumed to be independant of the type of isotope considered.

Table 3.3. Deposition parameters for the minimum deposition case.

Dry deposition parameter, v_d [cm/s]

Stability / Windspeed [m/s]	A	B	C	D	E	F
u < 1	0.01	0.01	0.01	0.01	0.01	0.01
1<=u< 3	0.01	0.01	0.01	0.01	0.01	0.01
3<=u< 6	0.01	0.01	0.01	0.01	0.01	0.01
6<=u<10	0.01	0.01	0.01	0.01	0.01	0.01
10<=u	0.01	0.01	0.01	0.01	0.01	0.01

Wet deposition parameter, l_g [sec^{-1}]

Stability	A	B	C	D	E	F
l_g [sec+-1]	2.0E-7	2.0E-7	2.0E-7	2.0E-7	2.0E-7	2.0E-7

Table 3.4. Deposition parameters for the normal deposition case 1.

Dry deposition parameter, v_d [cm/s]

Stability / Windspeed [m/s]	A	B	C	D	E	F
u < 1	0.4	0.3	0.3	0.2	0.07	0.05
1<=u< 3	1.0	1.0	1.0	0.7	0.3	0.2
3<=u< 6	1.0	1.0	1.0	1.0	0.6	0.4
6<=u<10	1.0	1.0	1.0	1.0	1.0	0.7
10<=u	1.0	1.0	1.0	1.0	1.0	1.0

Wet deposition parameter, l_g [sec^{-1}]

Stability	A	B	C	D	E	F
l_g [sec+-1]	3.9E-5	3.9E-5	4.1E-5	4.4E-5	3.6E-5	3.5E-5

Table 3.5. Deposition parameters for the normal deposition case 2.

Dry deposition parameter, v_d [cm/s]

Stability / $\overline{\text{Windspeed}}$ [m/s]	A	B	C	D	E	F
u < 1	0.4	0.3	0.3	0.2	0.07	0.05
1<=u< 3	1.6	1.4	1.2	0.7	0.3	0.2
3<=u< 6	2.0	2.0	2.0	1.5	0.6	0.4
6<=u<10	2.0	2.0	2.0	2.0	1.8	0.7
10<=u	2.0	2.0	2.0	2.0	2.0	1.6

Wet deposition parameter, l_g [sec^{-1}]

Stability	A	B	C	D	E	F
l_g [sec+-1]	3.9E-5	3.9E-5	4.1E-5	4.4E-5	3.6E-5	3.5E-5

Table 3.6. Deposition parameters for the maximum deposition case.

Dry deposition parameter, v_d [cm/s]

Stability / $\overline{\text{Windspeed}}$ [m/s]	A	B	C	D	E	F
u < 1	5.0	5.0	5.0	5.0	5.0	5.0
1<=u< 3	5.0	5.0	5.0	5.0	5.0	5.0
3<=u< 6	5.0	5.0	5.0	5.0	5.0	5.0
6<=u<10	5.0	5.0	5.0	5.0	5.0	5.0
10<=u	5.0	5.0	5.0	5.0	5.0	5.0

Wet deposition parameter, l_g [sec^{-1}]

Stability	A	B	C	D	E	F
l_g [sec+-1]	1.0E-4	1.0E-4	1.0E-4	1.0E-4	1.0E-4	1.0E-4

3.6. Parameters for dose calculations

The dose calculations are based on the meteorological parameters specified in 3.5 and the following assumptions:

Inhalation doses

During the overhead passage of the plume, a person standing on the ground will inhale an amount of radioactive material proportional to the passage time and the concentration at the location in question.

The total inhalation dose integrated over a given period of time after the activity is inhaled is calculated by multiplying the amount of each radionuclide inhaled with a dose-conversion factor for this particular radionuclide, and then adding these products.

The dose-conversion factor for a given radionuclide is equal to the dose per unit intake (in, e.g. Bq) integrated over a given period of time after the intake.

The inhalation doses are reduced by the filtration effect of houses. Here a reduction factor of 0.2 for filtration is used. This has been derived from recent Danish investigations (see Gjørup and Roed, 1980).

External dose from the plume

The decay of radionuclides is associated with the emission of radiation in the form of γ-photons.

The external γ-dose from the cloud is calculated by assuming that the cloud is composed of an infinite number of point sources and deriving the total dose by integration. Attenuation and multiple scattering of the γ-rays in the air are included in

the calculation of the dose from each point source. The γ-dose in the air is equal to the γ-flux density multiplied by the mass energy absorption coefficient for each of eight γ-energy groups.

Inside buildings, the external gammadose from the plume will be reduced considerably due to the shielding effect of the structure. In this report it is assumed that people remain indoors in brick buildings 89% of the time and outdoors the rest of the time.

A shielding factor of 0.76 has therefore been applied. This factor is given in WASH-1400 as representative of single-family houses and multi-storey brick buildings.

External dose from deposited activity

The external γ-dose from deposited activity is calculated by the same principles as the external dose from the plume; the ground is divided into a number of point sources and their dose contributions are integrated. By convention the dose in air is calculated at a point 1 m above the ground.

In this study it is assumed that people are outdoors 11% of the time and indoors the rest of the time. A shielding factor of 0.0769 is assumed in accordance with Gjørup (1981).

Total dose to the whole body

The long-term consequences of irradiation to the whole body is assessed from the committed effective dose equivalent. This is calculated here as the sum of:

1. The external gamma dose from the cloud.

2. The external gamma dose from deposited radionuclides integrated over 30 years.

3. The committed effective dose equivalent from inhalation of radionuclides during cloud passage. The calculation of this dose equivalent is based on an integration of the internal effects over 50 years, and it follows ICRP recommendations as shown below.

The committed effective dose equivalent is defined as:

$$H50_B = \sum W_T \times H_{50T}$$

where

$H50_B$ = Committed effective dose equivalent

$H50_T$ = 50 years committed dose equivalent for target tissue (organ T)

W_T = Weigting factor for target organ T.
(The summation involves all body organs).

Data for H_{50B}, H_{50T}, and W_T have been taken from ICRP 30 (ref. ICRP79).

4. CALCULATION RESULTS

Calculation of individual and collective doses have been made for two release heights, 20 and 100 meters.

4.1. Doses for the release height 100 m

The doses to individuals for the release height 100 m are shown on Fig. 4.1-4.4.

The committed effective dose equivalent is dominated by the external gamma dose from airborne activity which in turn is dominated by the contribution from the noble gases. As the noble gases are considered non depositable deposition has a neglectable influence on the committed effective dose equivalent. The total dose decreases when deposition increases but the relative difference between the two extreme deposition cases (minimum and maximum) is less than 4 percent.

The relative contributions to the total committed effective dose equivalent from the two other dose components, inhalation and external gamma dose from deposited material are small but more sensitive to deposition rate.

In the case of minimum deposition the external gamma dose from deposition is almost 2 orders of magnitude below the inhalation dose. When the deposition rate increases the external gamma dose from deposition increases and so does the relative importance of it in relation to the inhalation dose.

In the case of maximum deposition the gamma dose from deposition exceeds the inhalation dose by almost an order of magnitude. The

gamma dose from deposition increases almost proportionally with the (dry) deposition rate. In the present case the increase from minimum to maximum is a factor of 490.

A comparison with the doses calculated for the release height 20 meters (Fig. 4.13) clearly indicates that the influence of deposition on doses is dependant on release height i.e. dry deposition is the dominating mechanism (wet deposition is independant of the release height).

Inhalation doses, being directly proportional to the concentration of airborne material, vary less with depositon rate than the gamma doses from deposited material do. However inhalation doses are more sensitive to deposition than the gamma doses from the plume. The decrease in inhalation doses is between a factor 1.1 and 2 dependant on downwind distance when deposition varies from minimum to maximum.

Inhalation doses decreases less with distance than the gamma doses from deposition do due to the depletion of the plume when it travels downwind. Thus the difference between inhalation doses and gamma doses from deposition decreases with distance as seen on e.g. Fig. 4.2.

The collective committed dose equivalent is almost insensitive to deposition rate as shown on Fig. 5. The total collective dose out to 50 kilometers from the release point is 5 manrem. It decreases with increasing deposition rate but the difference between the minimum and the maximum case is only about 1.7%.

4.2. Doses for the release height 20 m

The doses to individuals for the release height 20 m are shown on Fig. 4.10.

The pattern is almost the same as for the release height 100 meters i.e. the variation of both the total dose (committed effective dose equivalent) and the individual dose components with deposition rate is the same. Further are the relative contributions of the dose components to the total dose almost the same as for the height 100 meters. However the decrease in release height increases the effect of deposition. This is due to the fact that the plume "reaches the ground" closer to the release point when the release height is decreased. The distance where the concentration (inhalation dose) is at its maximum moves closer to the release point as it is seen when comparing e.g. Fig. 4.2 and 4.7.

The variation of doses with depostion rate and release height are illustrated in table 4.1 where the ratio between maximum and minimum deposition doses are given.

Table 4.1. The ratio between doses to individuals calculated for the maximum deposition case and the doses calculated for the minimum deposition case.

Dose component \ Distance from release point	0.75 km		45 km	
	Release height		Release height	
	20 m	100 m	20 m	100 m
Gamma from plume	0.99	1.0	0.91	0.94
Inhalation	0.81	0.99	0.43	0.60
Gamma from deposition	410	490	160	250
Committed effective dose equivalent	1.0	1.0	0.93	0.97

The effect of deposition on collective committed effective dose equivalent is larger when the release height is decreased to 20 meters as shown on Fig. 4.10. The total collective dose integrated out to 50 kilometers from the release point is about 7 manrem.

The difference between the minimum and maximum deposition case is 8.1 per cent.

The variation of doses with release height and deposition rate is illustrated on Figs. 4.11 to 4.17.

As mentioned earlier a decrease of release height enhance the effect of deposition. This applies for the total dose as well as for the individual dose components except the external gamma dose from deposition. The variation of the gamma dose from deposition is shown on Fig. 4.13 (doses to individuals), Fig. 4.14, and 4.15 (collective doses). It is evident that deposition rate has less effect on gamma doses from deposited material when the release height decreases.

When the release height is low (e.g. 20 meters) deposition and the depletion of the plume are relatively high close to the release point. An increase of the deposition rate will increase deposition close to the release point and at the same time increase depletion of the plume thus leaving less material to be deposited at larger distances. An increase of the release height will reduce the concentration of airborne material at ground level close to the release point and this in turn reduces both deposition and depletion of the plume. As a consequence a larger amount of airborne material is permitted to travel further downwind before it is deposited. Generally speaking depletion of the plume becomes of importance from the downwind distance where the concentration of airborne material at ground level is at its maximum. Applying this rule to the present example gives that deposition "starts" at a distance of less than 0.75 km when the release height is 20 meters and about 3 km when the release height is 100 meters.

Committed effective dose equivalent

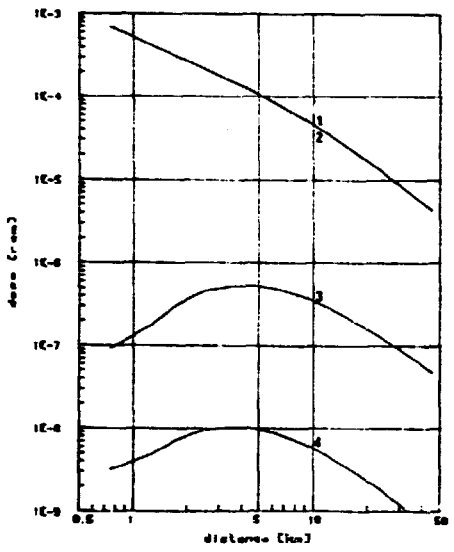

Fig.4.1

Minimum deposition

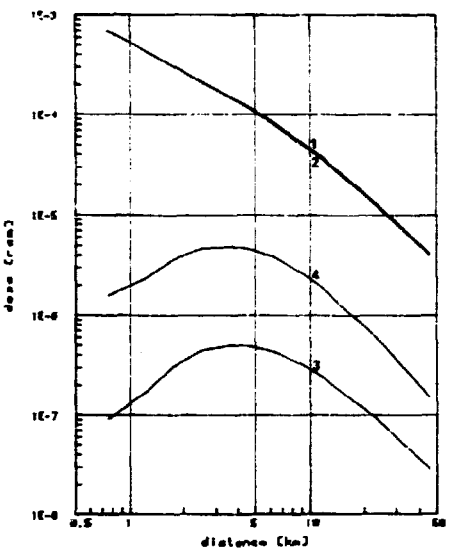

Fig. 4.2

Maximum deposition

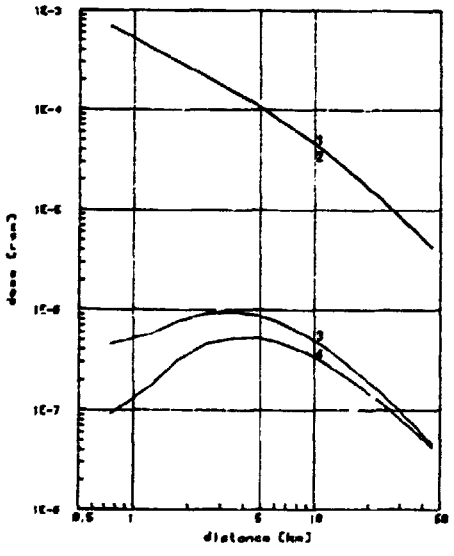

Fig.4.3

Normal deposition 1.

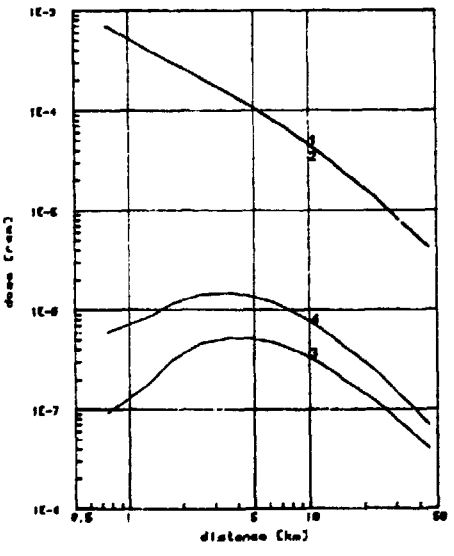

Fig.4.4

Normal deposition 2.

Release height: 100m

Doses from deposited material integrated over 30 y.

1. Total dose
2. External gamma dose from plume
3. Inhalation dose
4. External gamma dose from deposited material.

Collective committed effective dose equivalent

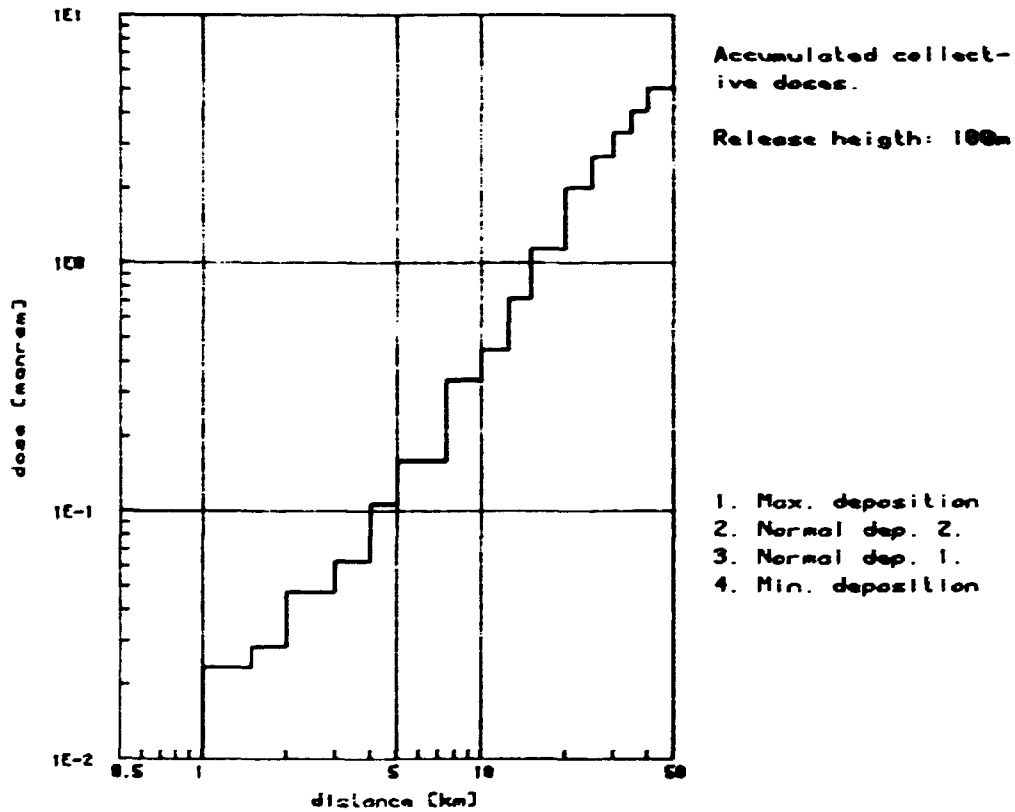

Fig. 4.5

Committed effective dose equivalent

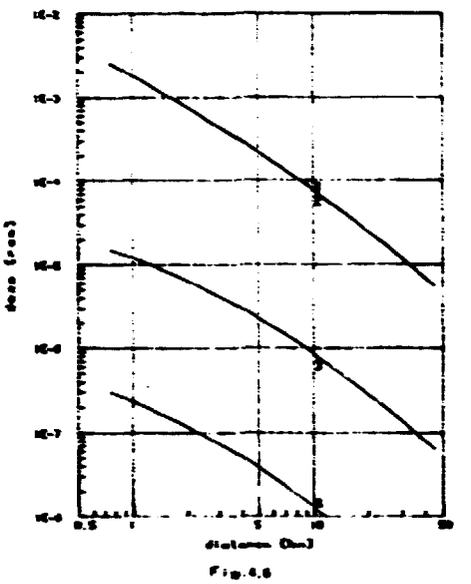

Fig. 4.6

Minimum deposition

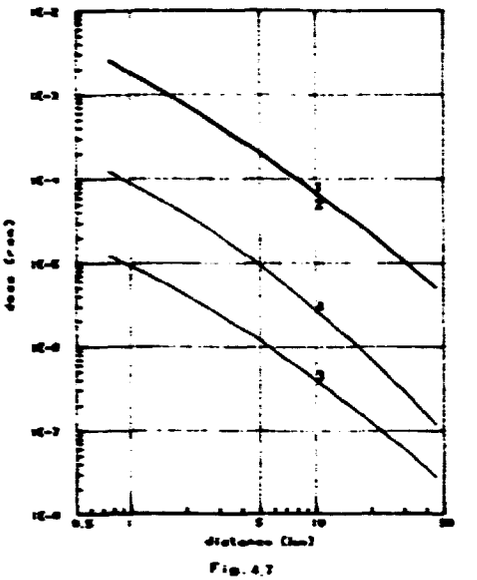

Fig. 4.7

Maximum deposition

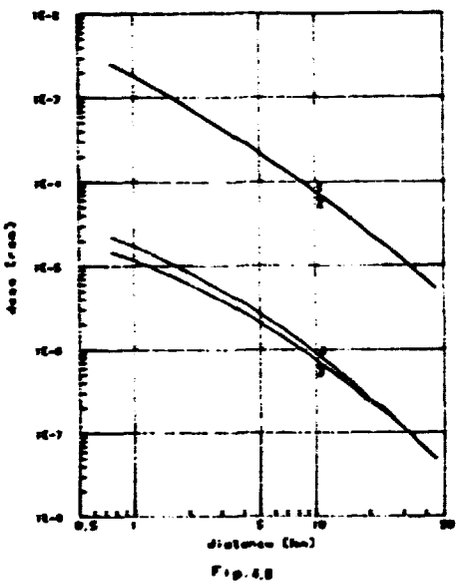

Fig. 4.8

Normal deposition 1.

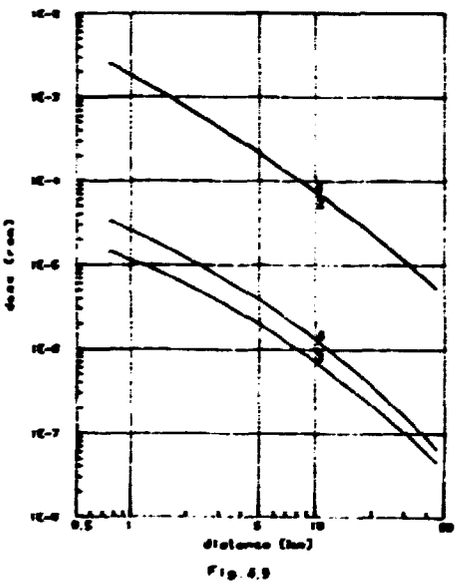

Fig. 4.9

Normal deposition 2.

Release heigth: 20m

Doses from deposited material integrated over 30 y.

1. Total dose
2. External gamma dose from plume
3. Inhalation dose
4. External gamma dose from deposited material.

Collective committed effective dose equivalent

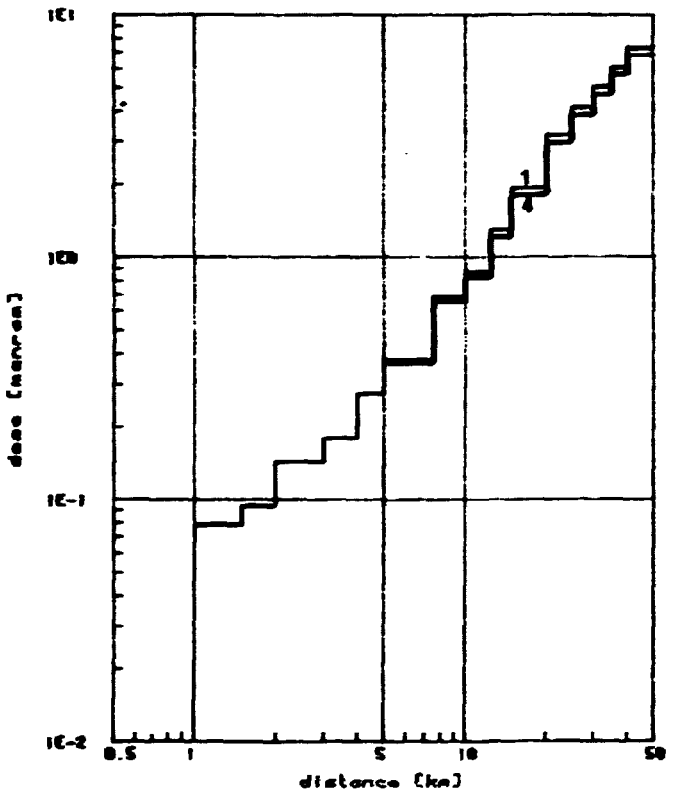

Accumulated collective doses.

Release heigth: 20m

1. Max. deposition
2. Normal dep. 2.
3. Normal dep. 1.
4. Min. deposition

Fig.4.10

External gamma dose from plume

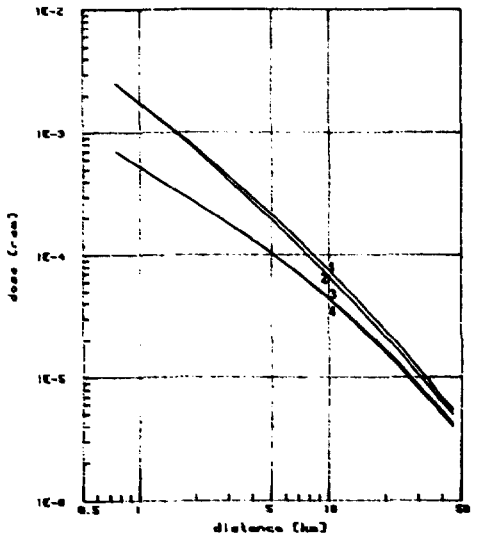

Fig.4.11

Inhalation dose

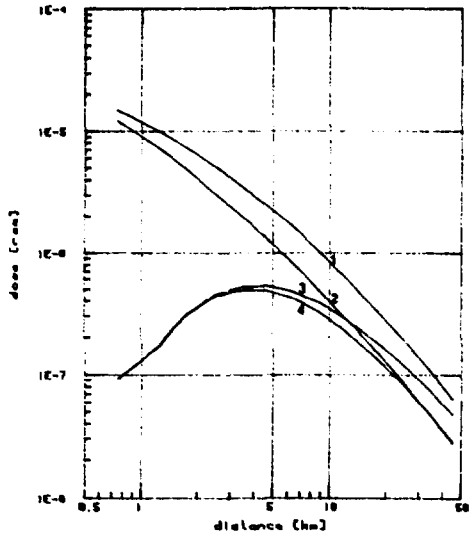

Fig.4.12

External gamma dose from deposited material. 30 y

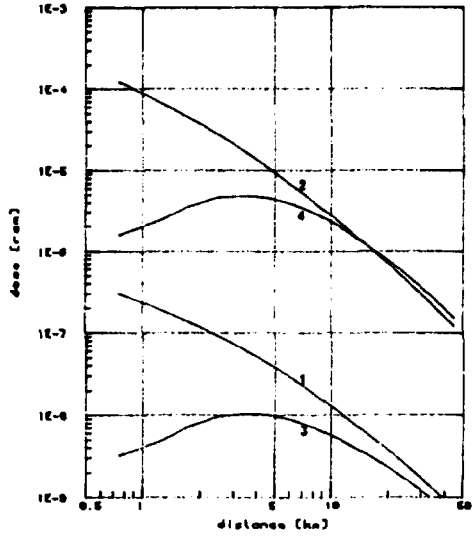

Variation of doses with deposition.

1. Min. dep. H= 20m
2. Max. dep. H= 20m
3. Min. dep. H= 100m
4. Max. dep. H= 100m

Fig.4.13

External gamma dose from deposition (30 y)

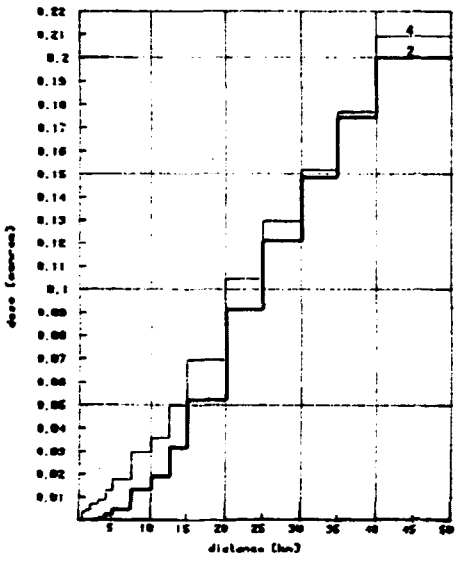

Fig.4.14

External gamma dose from deposition (30 y)

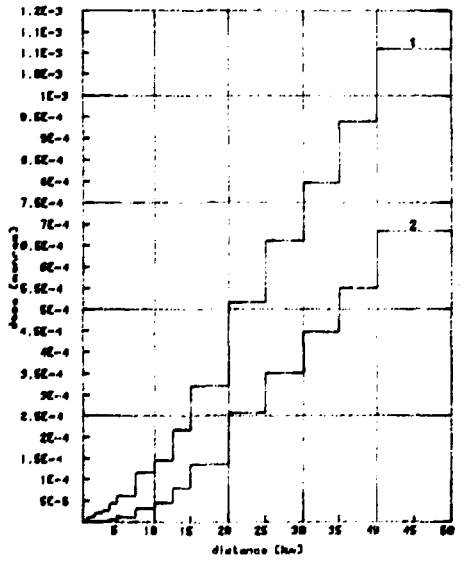

Fig.4.15

Committed effective dose equivalent

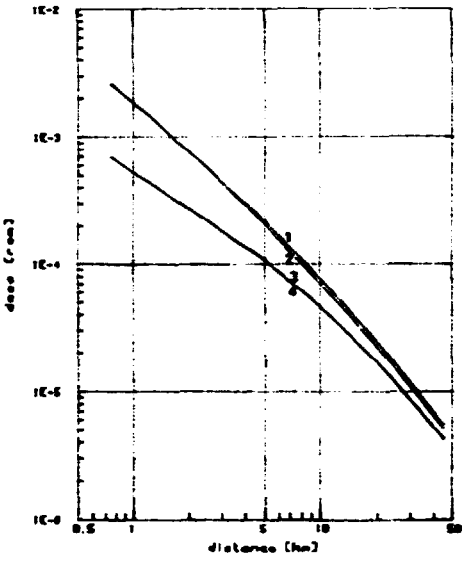

Fig. 4.16

Collective committed effective dose equivalent

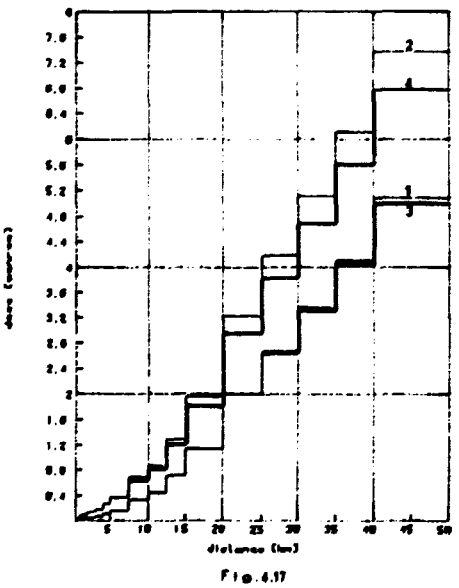

Fig. 4.17

5. CONCLUSION

Deposition, wet and dry, is found to be of minor importance to the committed effective dose equivalent (individual and collective) from annual routine releases to the air from a boiling water reactor (BWR). However, the choice of deposition parameters is of major importance for the assessment of the surface contamination and thus the radioecological consequences of airborne routine releases.

The long term doses from accidental releases are dominated by the external gamma doses from deposited material. Thus deposition is also of major importance in the case of accidents.

It is emphasized that the recommeded values of the dry deposition parameters (table 2.6 and "normal deposition 2") are maximum values. The actual values which should be used in the assessment of the consequences of a given release of material may be much lower. Furthermore the maximum v_D-values given are pertaining to a roughness length equal to 5 cm. A significant change of the roughness length will entail a significant change of the maximum v_D-values.

The recommended values for the wash-out coefficients (table 2.13) only applies for the average rain intensity in each stability class. As the wash-out coefficient increases when the rain-intensity increases the values used in a specific meteorological situation should be adjusted according to the actual rain intensity.

6. AKNOWLEDGEMENT

One author (SEL) aknowledges usefull discussion with N.O. Jensen at Risø.

REFERENCES

ALLERUP, P. and MADSEN, H. (1979). Accuracy of point precipitation measurements. Danish Meteorological Institute, Climatological papers No. 5.

BEATTIE, J.R. and BRYANT, P.M., (1973). Assessment of environmental hazards from reactor fission product releases. United Kingdom Atomic Energy Authority, Safety and Reliability Directorate. AHSB(S), R 135.

BRUTSAERT, W., (1975). The roughness length for water vapour, sensible heat and other scalars. Journ. Atm. Sci. 32, pp. 2028-2031.

BRYANT, P.M., (1966). Derivation of working limits for continuous release rates of ^{90}Sr and ^{137}Cs to atmosphere in a milk producing area. Health Physics 12, 1393-1405.

BUSCH, N.E., (1973). On the mechanics of atmospheric turbulence. In: Workshop on Micrometeorology (Ed. D.A. Hangen), American Meteorological Society, Boston, 1-65.

BUSINGER, J.A., WYNGAARD, J.C., IZUMI, Y., and BRADLEY, E.F., (1971). Flux-profile relationships in the atmospheric surface layer, Journ. Atmos. Sci. 28, pp. 181-189.

DYER, A.J., and HICKS, B.B., (1970). Flux gradient relationships in the constant flux layer. Quart. J. Roy. Met. Soc., 96, pp. 715-721.

ENGELMANN, R.J., (1968). Deposition of particles and gases. In: Meteorology and Atomic Energy (Ed.: D.H. Slade), pp. 108-221.

GARRAT, J.R., and HICKS, B.B., (1973). Momentum, heat and water vapour transfer to and from natural and artificial surfaces. Quart. J.R. Met. Soc. 99, pp. 680-687.

GOLDER, D., (1972). Relations among stability parameters in the surface layer. Bound. Lay. Met. 3, pp. 47-58.

GYLLANDER, C., and WIDEMO, U., (1980). Våtdeposition - aerosoler, et litteratur studie. Studsvik Arbetsrapport, K2-80/271.

JENSEN, N.O., (1973). Occurences of stability classes, wind speed, and wind directions as observed at Risø. Risø-M-1666.

JENSEN, N.O., (1981). A Micrometeorological perspective on deposition. Health Physics 40, pp. 887-891.

JENSEN, N.O., KRISTENSEN, L., and Petersen, E.L., (1982). Meteorology. In: Nuclear site evaluation for Carnsore Point. Unpublished.

KLUG, W., (1969). Ein Verfahren zur Bestimmung der Ausbreitungsbedingungen aus Synoptischen Beobachtungen. Staub-Reinhalt. Luft, 29, pp. 143-147.

KRETZSCHMAR, J.G., and Mertens, I., (1980). Influence of the turbulence typing schemes upon the yearly average ground-level concentrations calculated by means of a mean wind direction model. Atmos. Environ. 14, pp. 947-951.

LARSEN, S.E. and JENSEN, N.O., (1982). Summary and interpretation of some Danish climate statistics. Risø-R-399.

MAHRT, L., TROEN, I., and HEALD, R.C. A statistical variation of wind speed in the lowest few hundred meters. To be published.

NIELSEN, O.J., (1982). A litterature review on radioactivity transfer to plants and soil. Risø-R-450.

NIEUWSTADT, F.T.M., van ULDEN , A.P., (1978). A numerical study on the vertical dispersion of passive contaminants from a continuous source in the atmospheric suface layer. Atmos. Environ. 12, pp. 2119-2124.

PAULSON, C.A., (1970). The mathematical reprecentation of wind and temperature profiles in the unstable surface layer. Journ. Appl. Meteor. 9, pp. 857-861.

THYKIER-NIELSEN, S., (1980). The Risø model for calculating the consequences of the release of radioactive material to the atmosphere. Risø-M-2214.

USAEC, (1973). Reports on releases of radioactivity in effluents and solid waste from nuclear power plants for 1972. USAEC, Directorate of Regulatory Operations, Washington.

WASH-1258, (1973). Final environmental statement concerning proposed rule making action: Numerical guides for design objectives and limiting conditions for operation to meet the criterion "as low as practicable" for radioactive material in light-water-cooled nuclear power reactor effluents, volume 2. USAEC, July 1973.

WEBB, E.K., (1979). Profile relationships: The log-linear range, an extension to strong stability. Quart J. Roy. Met. Soc. 96, pp. 67-90.

Risø National Laboratory **Risø-M-2205**

Risø-M-2205

Title and author(s)

The Importance of Deposition for Individual and Collective Doses in Connection with Routine Releases from Nuclear Power Plants

Søren Thykier-Nielsen and Søren E. Larsen

Date April 1982

Department or group

Health Physics and Physics

Group's own registration number(s)

56 pages + tables + illustrations

Abstract

Deposition velocities, v_D, and wash-out coefficients, l_g, to be used in different velocity- and Pasquill classes in Denmark are estimated.

The estimated v_D's describe the maximum dry deposition possible, as the surface is assumed a perfect absorber in the considerations. The l_g-values are found corresponding to the average rain intensity, when it rains, within each Pasquill class and apply for materials which dissolve rapidly in water. The estimated parameter values were used as central values in a parameter study as follows:

For four different deposition cases and two release heights the committed effective dose equivalent (individual and collective) from a postulated annual routine release to the atmosphere has been calculated. An increase of the deposition parameters by more than one order of magnitude was found to have negligible influence on the total committed effective dose equivalent. However, the choice of deposition parameters was found to be of major importance for the assessment of the surface contamination and thus the radiological consequences of airborne routine releases.

Available on request from Risø Library, Risø National Laboratory (Risø Bibliotek), Forsøgsanlæg Risø), DK-4000 Roskilde, Denmark
Telephone: (03) 37 12 12, ext. 2262. Telex: 43116

Copies to